18th Brazilian Congress of Thermal Sciences and Engineering
November 16-20, 2020 (Online)

ENC-2020-0333

VERTICAL AXIS WIND TURBINE SAVONIUS STATIC ROTOR AERODYNAMIC COEFFICIENTS VALIDATION WITH OPENFOAM

Daniel Borges dos Santos

Edis Antunes Pinto Junior
Crístofer Hood Marques
Jeferson Avila Souza
Universidade Federal do Rio Grande – FURG, Escola de engenharia, Av. Itália, Km 8, S/N, CEP 96203-900, Rio Grande, RS, Brasil.
danielbsantoseng@gmail.com, edis.antunes@hotmail.com, cristoferhood@gmail.com, jasouza@furg.br.

Abstract. *In this work, a vertical axis wind turbine Savonius type is computationally simulated on its static state at different positions, rotating the rotor at six different angles, from 0 to 150 degrees. The objective is to find the aerodynamic forces coefficients applied to the rotor, torque, lift and drag coefficients, and determine a range of the optimal positions which it could start operating without the use of external devices. The numerical simulation and all geometry generation are done by free and open source software. The code used is OpenFOAM; it is based on Finite Volume Method and computes the pressure and velocity fields of the flow to calculate the forces acting on the rotor buckets. The results are validated comparing with other published articles.*

Keywords: *VAWT, Savonius rotor, OpenFOAM, numerical modeling*

1. INTRODUCTION

The Savonius wind rotor was patented in 1930 by the Finnish engineer Sigurd J Savonius (Savonius, 1930). It has a simple and easy to build design that has a high starting torque and low operating speed that results in less noise and wear of its moving parts. The acceptance of winds coming from any direction does not require turbine orientation devices as it is necessary in aerogenerators with horizontal axis. On the other hand, this device does not have the same efficiency as such aerogenerators. This is due to its components being closer to the ground, where wind currents are less intense and the tower is subject to high mechanical stresses. This device is indicated for urban environments where the flow can be turbulent in regions where they have several obstacles, not preventing its operation (Blackwell et al., 1977; Menet et al., 2013; Mereu et al., 2017).

To analyze this device, it will be used a numerical modeling tool, more specifically, computational fluid dynamics (CFD). CFD is the area of scientific computation that studies ways to solve real physical problems, involving the movement of fluids with or without heat transfer. It uses mathematical and computational resources to make known information such as pressures and velocities of the problems under study (Maliska, 2004). This study makes it possible to predict the positions of higher starting torque to know the positions with higher rotor torque and ensure that it is greater than the resistant torque to start the rotor (Nasef et al., 2013).

The Savonius turbine has been the subject of study for almost a century, during this period several changes were made to its geometry and operating conditions in search of improvements (Blackwell et al. 1977; Zamani et al. 2016). Due to the low performance of vertical axis wind turbines, it is an option to couple different devices to make better use of different specialties. For example, one of the ways to take advantage of the Savonius rotor's self-start feature is by applying it as a double stage coupled to the Darrieus rotor that has a higher peak power. Zamani and Maghrebi (2016), conducted a study using the OpenFOAM code, making geometric changes to the Darrieus turbine blades in order to, among others, improve the starting torque of the rotor. Several similar studies are also carried out with the Savonius turbine, changes in the bucket geometry such as the use of twisted blades, different flow values, and or variations in geometry such as the overlapping of buckets on the rotor directly affect these properties. The numerical tool, CFD, is a more economical way to test these variations and thus analyze quantitatively and qualitatively if properties such as aerodynamic efficiency and or if self-start had an increase in the rotor or not (Fujisawa, 1992; Saha and Rajkumar, 2006; Nasef et al., 2013; Menet and Rezende, 2013; Akwa et al., 2012).

Thus, the objective of this work is to perform a numerical evaluation on the torque, drag and lift coefficients of a Savonius turbine in static state, varying the position of this rotor, every 30 degrees, from 0 to 150 degrees using the open source code OpenFOAM. Then, the results obtained are compared with what was found by Oliveira et al., (2016) and Akwa (2010) to validate the model.

2. PROBLEM DESCRIPTION

Figure 1a presents the Savonius rotor geometry. There are two separated semi-circular blades with radius 0.544 m spaced by *s* and *a*. The *s* spacing is also called overlap ratio and it can be calculated as a function of the diameter, *s/D* while *a* is null. The turbine diameter is D = 1 m. The present work, following the recommendations of Fujisawa (1992) and Akwa et al., (2012), uses an overlap ratio of 0.15. To represent the external flow passing through the rotor, it will be made a plain cut in the 3 dimensional domain representing a cross section of the rotor into a wind tunnel as shown in Fig. 1b. According to Akwa (2010), Ferrari et al., (2017) and Menet et al., (2013), the 2D representation is in good agreement with the experiment of a Savonius rotor inside of a wind tunnel.

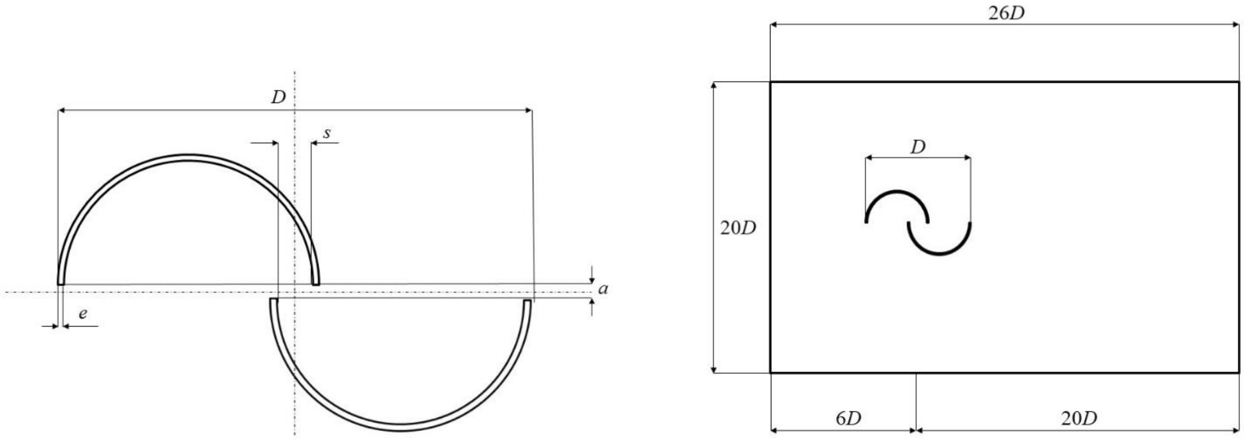

(a) (b)

Figure 1. Problem description: a) Savonious rotor, b) Computational domain.

2.1 Performance parameters

In the present work, all simulations were conducted using a Reynolds number equal to 4.33×10^5, calculated from the turbine diameter, D [m], fluid viscosity, ν [m²/s] and flow velocity U_{inf} [m/s]. This value was taken from the work of Akwa (2010) which is based on Blackwell's (1977) experiment.

$$Re = \frac{D\,U_{inf}}{\nu} \tag{2}$$

The static torque coefficient, C_m, can be calculated according to

$$C_m = \frac{M}{\frac{1}{4}\rho U_{inf} D} \tag{3}$$

where M is the static torque [N m] and ρ is the air density [kg/m³].

The drag and lift forces are responsible for the Savonius turbine operation. In Fig. 2, is shown these forces acting on the turbine rotor, U_{tan} is the tangential velocity which considers the rotor radius and angular velocity, U_{rel} is the relative flow velocity over the blade, α represents the attack angle of the relative flow over the blade and F_{res} is the resulting force acting over the blade. All acting forces are affected by the angular position of the blade, θ, and by the rotation effects of the turbine and changing the angular position of the rotor will affect all forces acting on it.

$$U_{rel} = U_{inf} - U_{tan} \tag{1}$$

Also, it is possible to describe drag and lift coefficients, C_d and C_l according to

$$C_d = \frac{F_d}{\frac{1}{2}\rho A U_{inf}^2} \tag{4}$$

$$C_l = \frac{F_l}{\frac{1}{2}\rho A U_{inf}^2} \tag{5}$$

where F_d is the drag force, F_l is lift force and A is the frontal area of the rotor.

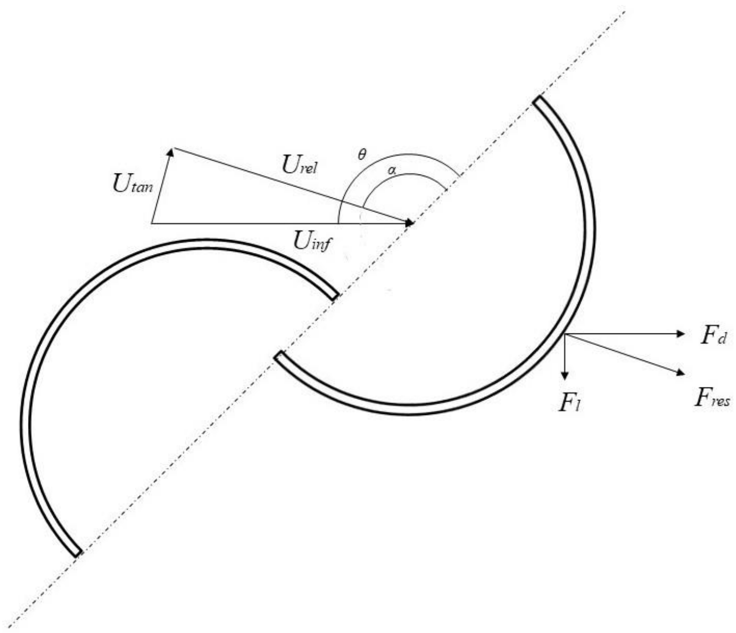

Figure 2. Forces acting at Savonius rotor.

2.2 Numerical model

To solve an incompressible fluid flow on steady and turbulent regime it was used the Reynolds-Average Navier Stokes (RANS) model to solve the mass and momentum balance equations and the turbulence transport equations. To model the turbulence, it was used the eddy-viscosity model k-ω SST (Menter, 1993). The simulation is solved on steady regime using the solver simpleFoam (Holzmann, 2017), to solve the pressure-velocity coupling problem, from OpenFOAM software on its version 7.

The mass balance equation can be described as

$$\frac{\partial \rho}{\partial t} + \nabla \cdot (\rho V) = 0 \tag{6}$$

where ρ is density [kg/m³], t is time [s], and $\boldsymbol{V}$ is the velocity field [m/s].

And the momentum equation is

$$\frac{\partial (\rho V)}{\partial t} + \nabla \cdot (\rho V V) = -\nabla p + \nabla \cdot \tau + \rho g + F \tag{7}$$

where p is pressure [Pa], $\boldsymbol{g}$ the gravity vector [m/s], $\boldsymbol{F}$ the force term [N/m³] and τ the stress tensor [Pa].

Boundary conditions are also shown in Fig. 3. Constant flow velocity is prescribed at the left face (inlet), full developed flow (null derivative of all variables in the flow direction) is set at the right side face (outlet) and symmetry is specified to top and bottom faces. As OpenFOAM requires a tridimensional mesh to run, it provides a boundary condition called empty, used to indicate the non specified domain limits of a 3 dimensional geometry. Besides, mesh should have only one volume in this direction.

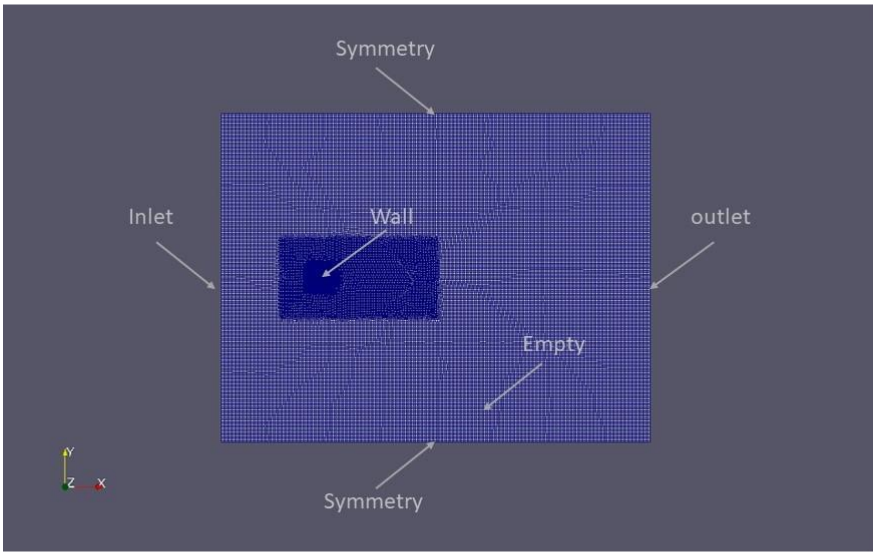

Figure 3. Boundary conditions.

2.3 Mesh and domain

A grid convergence analysis (GCA) was performed in order guarantee results quality along with reducing the number of cells in the domain. Figure 3 shows the computational domain of the proposed problem, as well as, the imposed boundary conditions. Figures 4a and 4b show the details of the mesh in the region close to the rotor blades. This region requires a controlled domain of minimum distance of the first meshing element close to the blade walls. According to Cebeci (2013), the parameter used to control mesh quality in this distance is called Y+, which suggests that a Y+ less than approximately 5 is a good approximation for turbulence model k-ω SST. Thus, to obtain such approximation details of the elements close to the rotor, refinement zones regions were used as shown in Fig. 3 and 4; one immediately next to the blades, important to obtain a low value of Y+ as shown in Fig. 4b, a second around the entire rotor, Fig. 4a, and one more external refinement used as a transition to the coarse mesh region located far from the blades, Fig. 3. The geometry and mesh were generated using the free software gmsh (Geuzaine and Remacle, 2009) and then exported to OpenFOAM.

To reduce computation time and keep accuracy in the results GCA is shown in Tab. 1. It represents the evaluation of the static torque, drag and lift coefficients for the 0 degree rotor position.

Table 1. Grid convergence analysis on 0 degree rotor position.

Name	Cells	Cm	Error*	Cd	Error*	Cl	Error*
Refined	203279	0.203	-	0.259	-	0.323	-
Medium	92740	0.186	8.37%	0.275	5.81%	0.323	0.00%
Coarse	50927	0.205	9.26%	0.272	1.09%	0.380	15.00%
*$(1 - C_{min} / C_{max}) \cdot 100$							

Thereby, based on the GCA, due to values being small, 10% error margin criteria were set. For time efficiency and acceptable error margin the medium refinement mesh was used to run the cases. This mesh has a Y+: min = 4.06374, max = 4.34618, average = 4.32792 coefficient which is acceptable for the k-ω SST model.

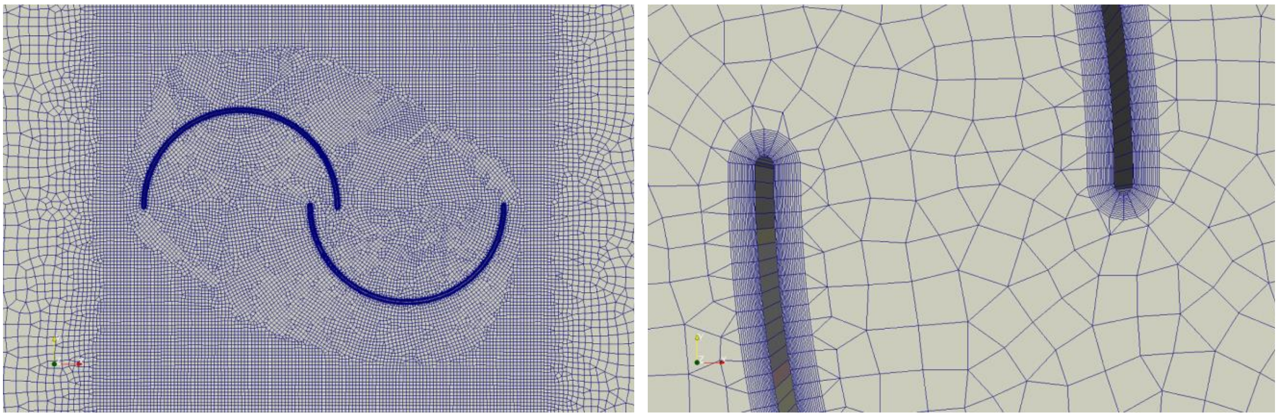

(a) (b)

Figure 4. Rotor meshing details: a) Refinement zone, b) Meshing layers.

3. RESULTS

A series of simulations have been caried out with the static Savonius rotor switching the angular position of the blade. In Figure 5 is shown the output for the static torque coefficient at every instant for the 0 degree position. So, to achieve the averaged C_m, a weighted time average is calculated such as

$$C_{m,ave} = \frac{1}{T}\int C_m dt \quad (8)$$

where, T is the integration interval [s], C_m is the instantaneous static torque and t is the time [s].

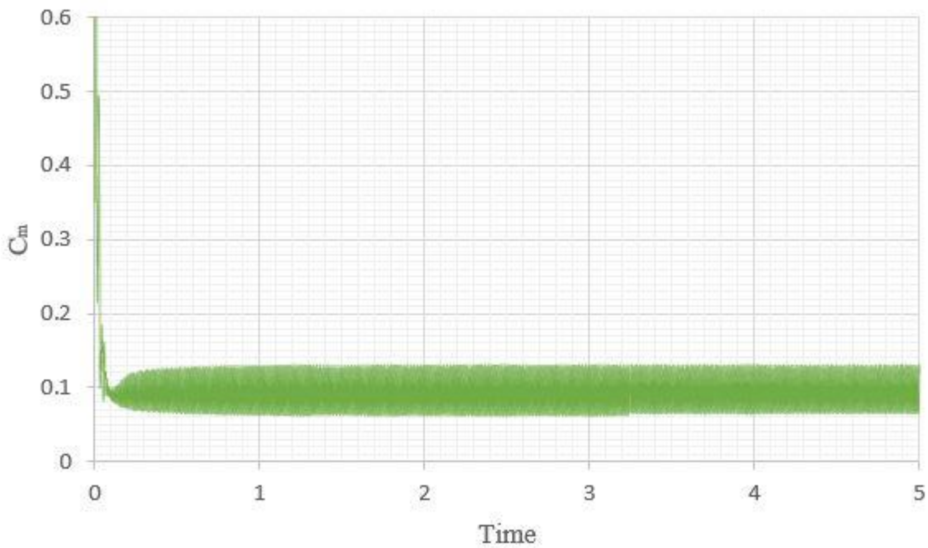

Figure 5. Instantaneous static torque (0 degree).

This procedure was used to all coefficients and the cases were compiled accordingly. The obtained velocity profiles are shown in Fig. 6 for t = 2 s.

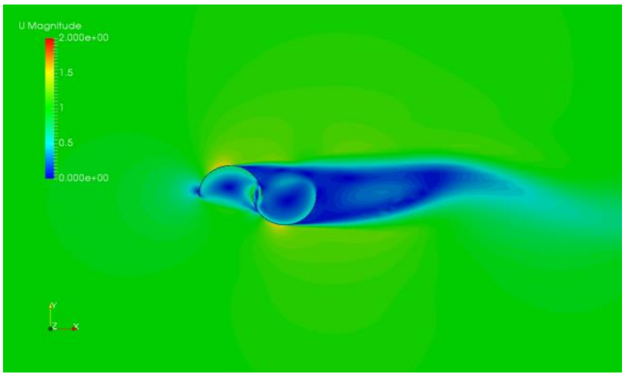

0 degree

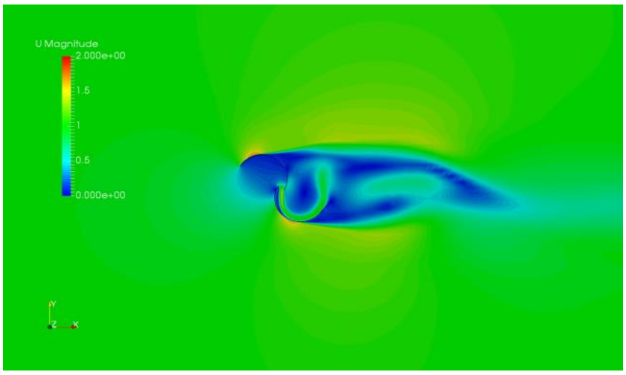

30 degree

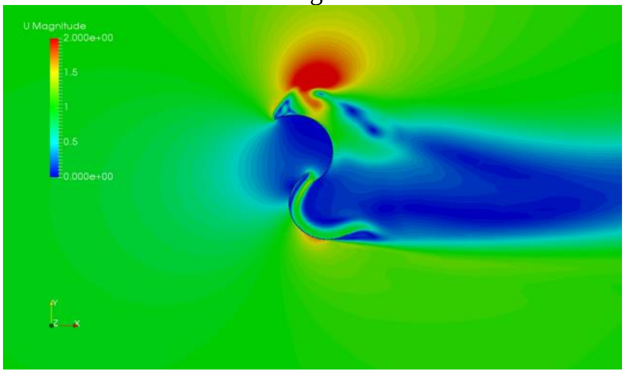

60 degree

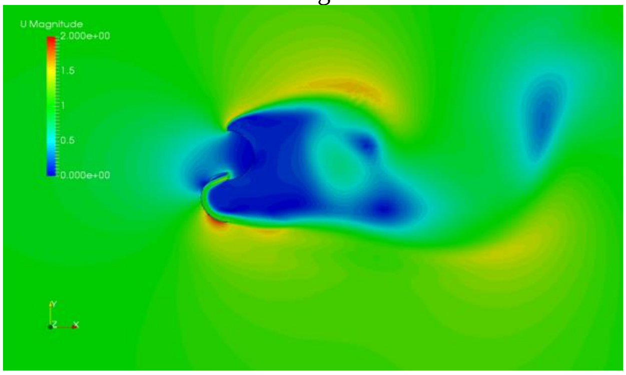

90 degree

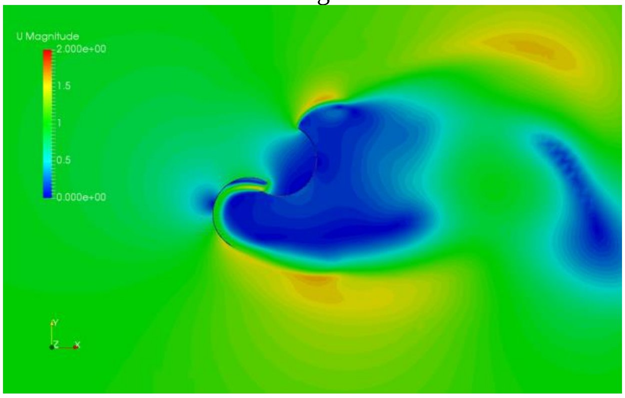

120 degree

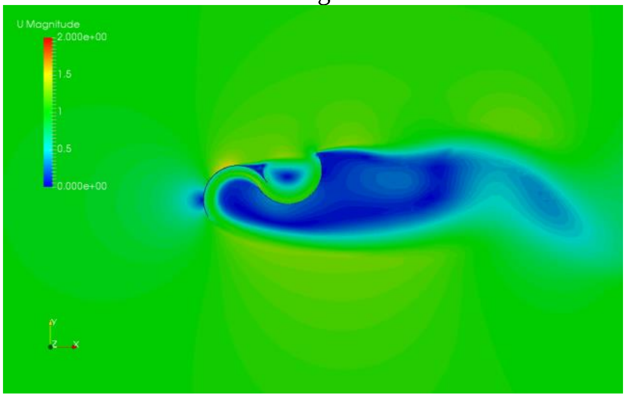

150 degree

Figure 6. Savonius rotor velocity gradients at 2 seconds time.

At this point the solution is already stable, however like Nakajima et al (2008) in Fig. 7, it is possible to see that there are still vortices happening and it is due the turbulent nature of the flow. Also, the high and low velocity zones are in agreement with what was expected and the obtained results now can be compared to other authors in order to validate the case.

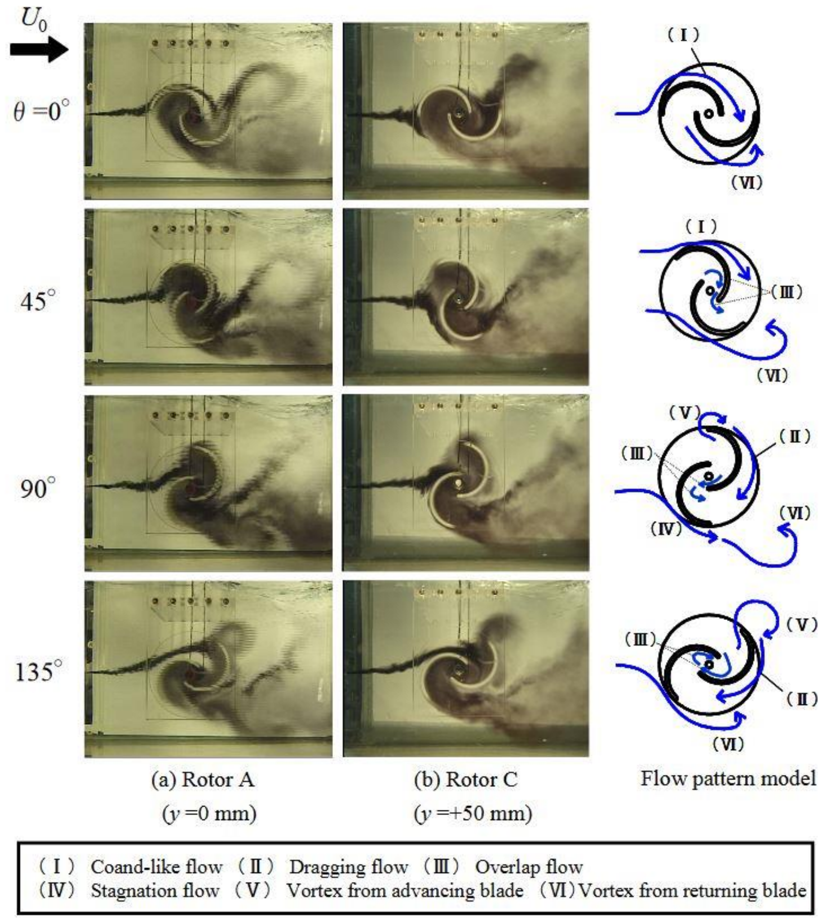

Figure 7. Flow patterns from y-axial view. (From: Nakajima et al., 2008)

In figures. 8-10 is shown a comparison of obtained coefficients with those presented by Akwa (2010) obtained using StarCCM+ and Oliveira et al. (2017) obtained using Fluent.

In both curves the static torque has a maximum at rotor angle from 30 to 60 degrees and a minimum at 120 to 180 degrees. For the drag coefficient the curve has a maximum at 90 to 120 degrees and a minimum at 0 to 30 degrees while for the lift coefficient curve it has a maximum at 0 to 30 degrees and a minimum at 90 to 120 degrees.

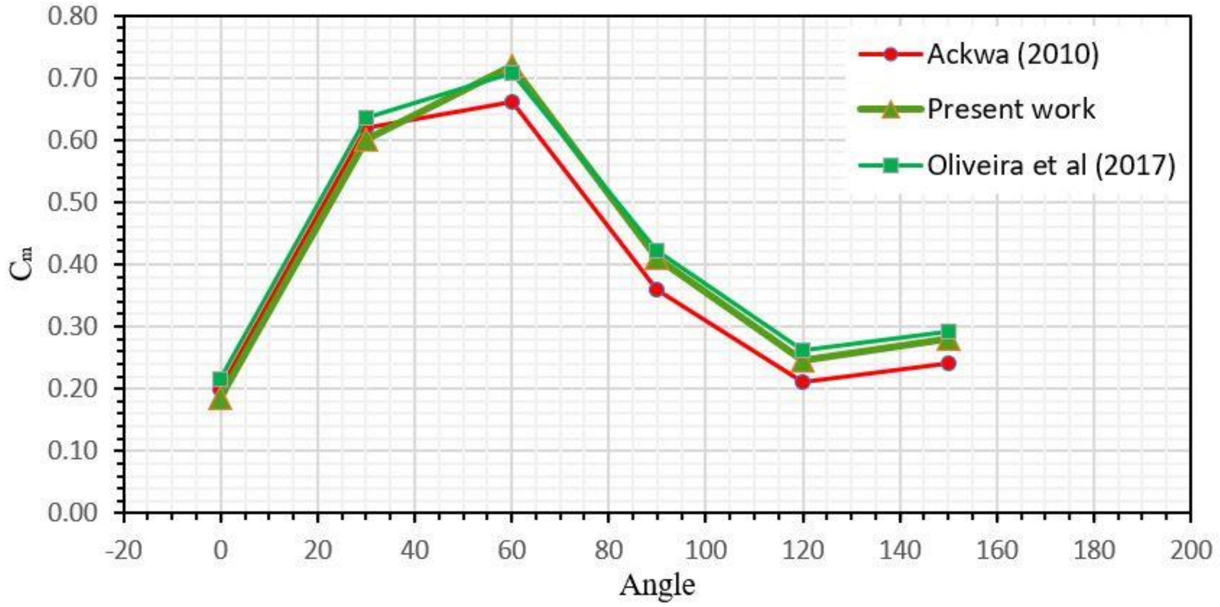

Figure 8. Static torque coefficient comparison.

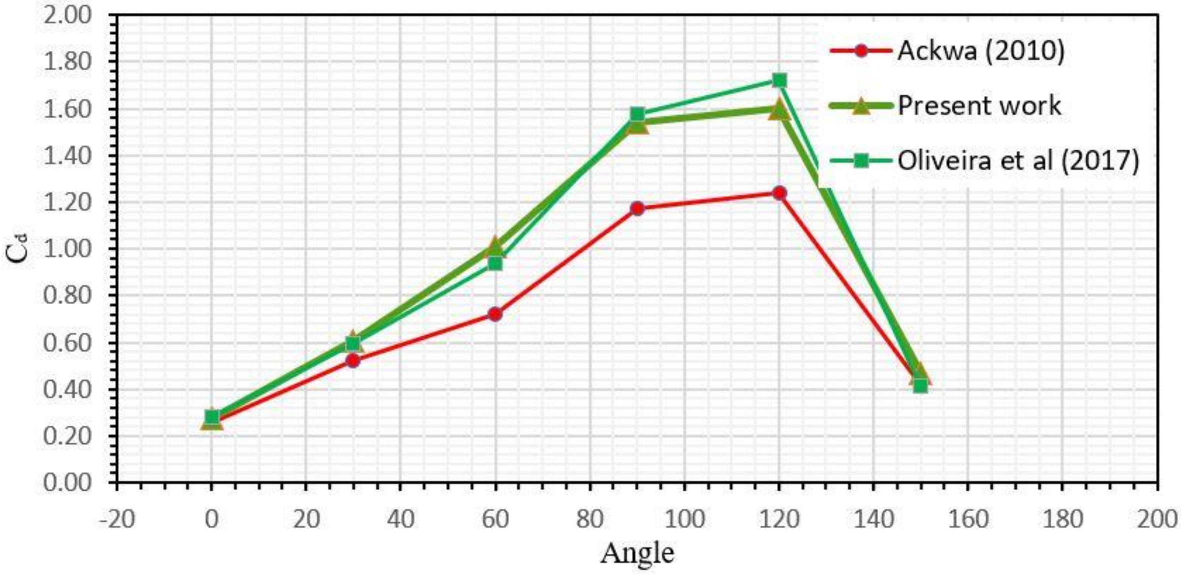

Figure 9. Drag coefficient comparison.

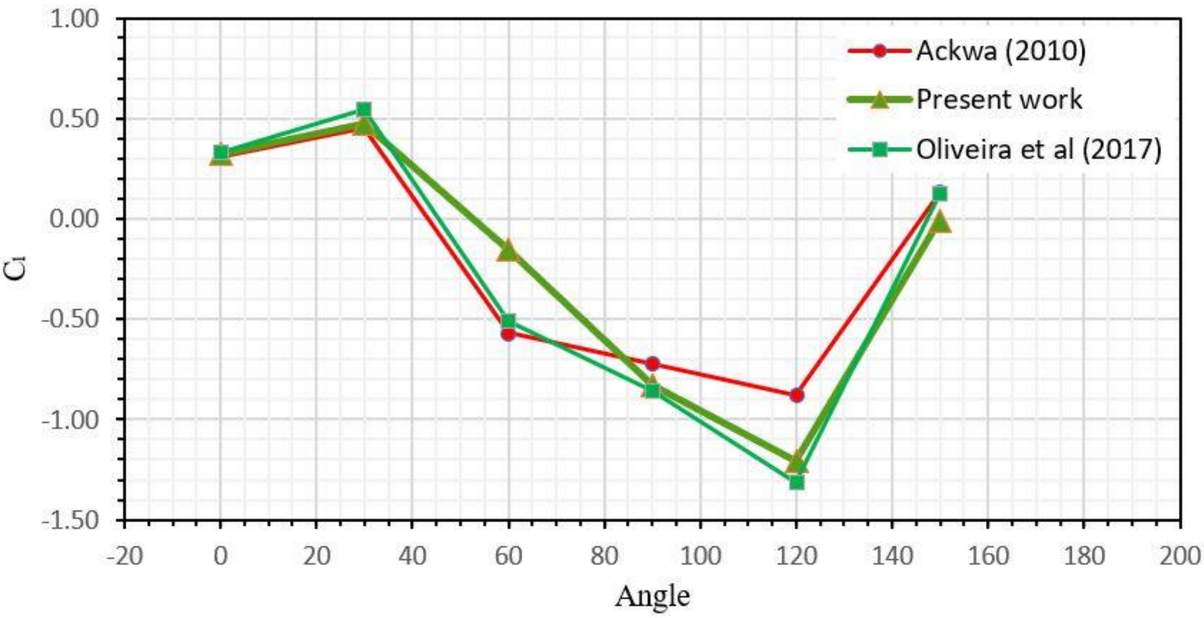

Figure 10. Lift coefficient comparison.

As shown in Figs. 8-10, all the coefficients have the same tendencies of behavior, however the present work results are closer to Oliveira et al., (2017). For the static torque the maximum difference is at 60 degrees comparing to Akwa (2010) for 8.90% and at 30 degrees for Oliveira et al., (2017) for 5.55%. For the drag coefficient the maximum difference occurs at 90 degrees, 31.54% comparing to Akwa (2010) and at 120 degrees, 7.06% comparing to Oliveira et al, (2017). Finally, the lift coefficient has a maximum difference at 60 degrees, 73.42% comparing to Akwa (2010) and also at 60 degrees, 70.36% comparing to Oliveira et al., (2017). The results found demonstrate coherence between all coefficients compared to the other authors.

4. CONCLUSIONS

In this article, a static Savonius rotor numerical modeling has been conducted. In order to validate the models presented with open source code OpenFOAM a grid was constructed with gmsh. The first part of meshing was a discretization of layers following the blades of the rotor, so it could have an acceptable Y+ for the turbulence model. Second, it had to have an optimization that lead to a 65% elements number reduction while maintaining good accuracy. Then the model has been validated comparing the aerodynamic coefficients with other articles, having shown good agreement in the results. So, with the results found in this work it is possible to say that this Savonius geometry can self-start at any static position, having its higher efficiency while the advance blade is at 30 and 60 degrees.

5. ACKNOWLEDGEMENTS

The author D. B dos Santos acknowledge CAPES for master scholarship (Finance Code 001) and J. A. Souza acknowledge CNPq for research grant process number 304699/2019-5.

6. REFERENCES

Akwa, J. V., 2010. *Análise aerodinâmica de turbinas eólicas Savonius empregando dinâmica dos fluidos computacional*. Msc Thesis, Universidade Federal do Rio Grande do Sul, Porto Alegre, Brasil.

Akwa, J. V., Silva Júnior, G., Petry, A., 2012. "Discussion on the verification of the overlap ratio influence on performance coefficients of a savonius wind rotor using computational fluid dynamics". *Renewable Energy*, Vol. 38, No. 1, pp. 141-149.

Blackwell B. F., Sheldahl, R. E., Feltz, L. V., 1977. "Wind tunnel performance data for two and three bucket savonius rotors". *Journal of Energy*, Vol 2, No. 3, pp. 160-164.

Cebeci, T., 2013. *Analysis of Turbulent Flows with Computer Programs*. Elsevier Ltd. Third edition.

Ferrari, G., Federici, D., Schito, P., Inzoli, F., Mereu, R., 2017. "Cfd study of savonius wind turbine: 3d model validation and parametric analysis". *Renewable Energy*, Vol. 105, pp. 722-734.

Fujisawa, N., 1992. "On the torque mechanism of Savonius rotors". *Jornal of Wind Engineering and Industrial Aerodynamicsi*, Vol. 40, No. 3, pp. 277-292.

Geuzaine, C., Remacle, J.-F., 2009. "Gmsh: A 3-D finite element mesh generator with built-in pre- and post-processing facilities". *International Journal for Numerical Methods in Engineering*, Vol. 79, No. 11, pp. 1309–1331.

Holzmann, T., 2017. *Mathematics, Numerics, Derivations and OpenFOAM®*. Copyright Tobias Holzmann, fourth edition.

Maliska, C. R., 2004. *Transferência de calor e mecânica dos fluidos computacional*. Livros Técnicos e Científicos Editora S/A, 2nd Edição Revisada e Ampliada.

Menet, J. L. Rezende, T., 2013. "Static and dynamic study of a conventional Savonius rotor using a numerical simulation". In *proceedings of the 21st Congres Français de Mecanique*. Bordeaux, France.

Menter, F. R., 1993. "Zonal two equation k-ω turbulence models for aerodynamic flows". *AIAA paper 2906*.

Mereu, R., Federici, D., Ferrari, G., Schito, P., Inzoli, F., 2017. "Parametric numerical study of Savonius wind turbine interaction in a linear array". *Renewable Energy*.

Nakajima, M., Iio, S., Ikeda, T., 2008. "Performance of Savonius Rotor for Environmentally Friendly Hydraulic Turbine". *Journal of Fluid Science and Technology*. Vol. 3, No. 3, pp. 420-429.

Nasef, M. H., El-Askary, W. A., AbdEl-hamid, A. A., Gad, H. E., 2013. "Evaluation of Savonius rotor performance: Static and dynamic studies". *Journal of Wind Engineering and Industrial Aerodynamics*, Vol. 123, pp. 1-11.

Oliveira, G. N., Rocha, L. A. O., Petry, A. P., Isoldi, L. A., Vieira, R. S., Santos, E. D., 2017. "Influência do refinamento de malha nos coeficientes de arrasto, sustentação e torque estático de uma turbina Savonius de único estágio." *Revista Brasileira de Energias Renováveis*, Vol. 6, No. 3, pp. 438-453.

Saha, U. K., Rajkumar, M. J., 2006. "On the performance analysis of Savonius rotor with twisted blades". *Renewable Energy*, Vol. 31, pp. 1776-1788.

Savonius, S. J., 1930. *Wind rotor.* uS Patent 1,766,765. (Jun. 24).

Zamani, M., Maghrebi, M. J., Varedi, S. R., 2016. "Starting torque improvement using J-shaped straight-bladed Darrieus vertical axis wind turbine by means of numerical simulation". *Renewable Energy*, Vol. 95, pp. 109-126.

7. RESPONSIBILITY NOTICE